High index contrast polysiloxane waveguides fabricated by dry etching

S. J. Madden,[a] M. Y. Zhang, D.-Y. Choi, and B. Luther-Davies
Laser Physics Centre, Research School of Physical Science and Engineering, Australian National University, Canberra ACT 0200, Australia

R. Charters
RPO Inc., Innovations Building, Australian National University, Canberra ACT 0200, Australia

(Received 12 December 2008; accepted 22 March 2009; published 28 April 2009)

The authors demonstrate the production of low loss enhanced index contrast waveguides by reactive ion etching of IPG™ polysiloxane thin films. The use of a silica mask and CHF_3/O_2 etch gas led to large etch selectivity between the silica and IPG™ of >20 and etch rates of >100 nm/min. This work indicates that compact optical circuits could be successfully fabricated for telecommunication applications using polysiloxane films. © *2009 American Vacuum Society.*
[DOI: 10.1116/1.3119670]

I. INTRODUCTION

Polymers have long been recognized as leading contenders for the fabrication of low cost integrated optical components, and polysiloxane based materials in particular have realized low loss planar waveguides[1–4] that have been commercialized and demonstrated to meet the stringent reliability requirements for deployment in carrier networks.[5,6] Polysiloxane waveguides compatible with SMF-28 optical fiber have been demonstrated using a negative resist like process with 6×6 μm cores and 0.3% index contrast,[1] and plasma etched 8×8 μm cores with up to 0.6% index contrast.[2–4] The modest index contrasts used to date preclude bend radii below 1 cm,[7] and are relatively insensitive to roughness on the waveguide surfaces due to both the low contrast and large size.[8]

It is well known that a key cost reduction measure is to scale down the die size for any given device, and in the case of optical devices, the waveguide bend radius and propagation loss are the factors that limit how far this may be taken. Minimum usable bend radius is a strong function of index contrast, and for waveguides with indices around those of typical polymers, it is necessary to reach an index contrast of ~2% to obtain around 1 mm bend radii.[7] This represents an increase in the index contrast of over three times that of all previously demonstrated polysiloxane waveguides. Concurrently the waveguide dimensions need to shrink by about a factor of 2 to maintain single mode operation.

These factors have two important implications for polysiloxane waveguides. Firstly, it is known that negative resist type processes for polysiloxanes encounter difficulties in patterning features below about 5 μm (Ref. 9) due to free radical diffusion beyond the exposed area, effectively removing that fabrication route and leaving plasma etching as a viable alternative. Secondly, given the sidewall scattering loss for a waveguide scales approximately as the square of the index contrast[10] and is impacted by decreases in the waveguide size,[8] then maintaining low loss requires very smooth sidewalls in order for roughness not to become the dominant loss factor. Given that plasma etching is the only demonstrated route to the dimensions required, this translates directly to etch quality.

Relatively little has been reported on etching of polysiloxane materials for waveguide applications. Usui *et al.*[3] gave only brief details on the masking and process chemistry/conditions and little detail of the sidewall roughness. Smiegal and co-workers[11,12] gave more detail but did not appear to attain roughness results that would be acceptable for waveguide applications. Aside from the etching itself, there is also an issue with masking. High reliability polysiloxane devices operate in the region where the material is above its glass transition temperature, i.e., in a rubberlike state. This means that the material is much softer than most inorganic materials usually used as hard etch masks, and this combined with the large coefficient of thermal expansion of polysiloxane materials can produce problems with wrinkling of the film.[13] Again little has been reported on this in a waveguide fabrication context.

In this article therefore we report on the production of enhanced index contrast ($\Delta n \approx 0.029$) polysiloxane waveguides with mode areas of between 12 and 20 μm^2 by plasma etching. We determined masking and etching conditions for a commercial polysiloxane material (IPG™ from RPO Inc.), which leads to surface roughness below 1 nm rms and optical losses below 0.8 dB/cm at 1550 nm and 0.4 dB/cm at 1310 nm.

II. ETCH MASK SELECTION AND FABRICATION

The selection of the mask layer is important in dry etching to ensure that sufficient selectivity is obtained for the required etch depth. Given that previous research showed the need for substantial amounts of oxygen in the etch gas,[2–4,11,12] then a mask or buffer layer that etches slowly in an oxygen/fluorocarbon gas mix is required because photoresist is likely to etch at a substantial rate in such a mixture. Moreover, a smooth, vertical profile is required in the mask

[a]Author to whom correspondence should be addressed; electronic mail: sjm111@rsphysse.anu.ed.au

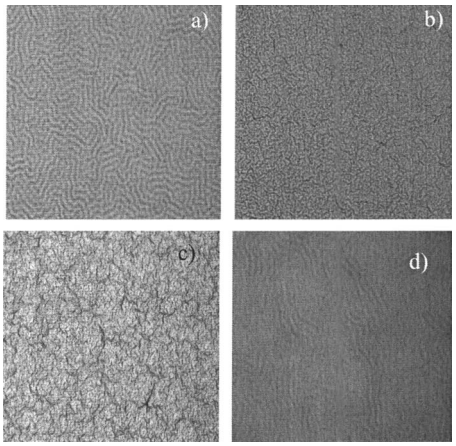

FIG. 1. Differential interference contrast optical microscope images of previously smooth aluminum films postbaking at 130 °C. Differing deposition conditions were used in (a)–(c). (d) shows the polysiloxane surface after the aluminum has been stripped revealing that the wrinkles have been permanently transferred to the polymer. Field of view is 70×70 μm^2 in all images.

itself, meaning generally it is advantageous if the mask/buffer layer material is itself dry etchable with high selectivity to the polysiloxane.

Typically hard etch masks used with fluorocarbon gas mixes are made from aluminum or chromium. While chromium is the standard material for photomasks and a lot of research and development has consequently gone into dry etching chrome; the process is not an easy one and is aggressive requiring high flows of chlorine and oxygen, something likely to attack polymers rapidly. Aluminum has the benefit of being easiest to dry etch at very high selectivity, while offering reasonable selectivity in fluorocarbon etches. Hence a sputtered aluminum mask was the first choice. As previously observed,[13] improper deposition conditions lead to wrinkling of the polysiloxane surface during metal deposition. Suitable conditions were found where the substrate was heated negligibly and this resulted in smooth as-deposited Al films on the polysiloxane surface. However, after the thermal treatment required for photoresist processing (baking at 90 and 110 °C), the film was found to wrinkle again. Figures 1(a)–1(c) show wrinkling of different severities in previously smooth 200 nm thick aluminum films deposited under different conditions after baking at 130 °C.

The wrinkles were found to occur if the film was heated above ~90 °C, and atomic force microscopy (AFM) indicated the peak to valley height of the features of up to 25 nm. Testing revealed that the wrinkling was not an oxidation induced issue nor an adhesion or film deposition related matter. Interestingly, the surface retained the wrinkle pattern even after removing the aluminum, as shown in Fig. 1(d). The reasons behind the wrinkling behavior are believed to be similar to those that result in "hillocking" in very large scale integration (VLSI) interconnects made from aluminum. Here compressive forces resulting from thermal expansion mismatches extrude the weakest crystal planes in the polycrystalline film. In the present case, the IPG™ material has a much greater thermal expansion coefficient than aluminum (600×10^{-6} versus $23\times10^{-6}/°C$), and rather than extrusion we believe we are seeing "drawing" of the aluminum at elevated temperatures, which upon cooling requires buckling of the film to release the newly generated compressive stress. We also tested chromium films. Chromium is well known for its tendency to deposit under high film stress, and we found that under a wide range of deposition conditions the film "cracked" into smooth platelets. Inspection revealed that we were able to cause this behavior with compressive or tensile stress in the chromium film. We were unable to find a sputtering condition in our apparatus that resulted in a low enough stress in the chromium film to prevent tearing of the polysiloxane surface.

The obvious answer to these problems was to insert either a mechanically strong buffer layer or one with coefficient of thermal expansion (CTE) intermediate to that of IPG™ and aluminum. Given limited material choices, we chose to use silicon dioxide deposited by either low temperature plasma-enhanced chemical vapor deposition (PECVD) or rf sputtering due to its high strength.[14] Films deposited by either technique 2–300 nm thick were successful at preventing the degradation of the aluminum film. However the greater level of processing complexity involved in a two layer mask system was not attractive, and we resolved to try and identify a process which would give the required etch selectivity using the silicon dioxide layer alone. Additionally a silicon dioxide mask does not need to be removed after etching as it is optically loss free, thereby eliminating the mask removal step. We, therefore, used a 300 nm thick layer of silicon dioxide deposited by rf sputtering, which was then coated with an ~1 μm thick standard positive resist (Clariant AZ 701 MiR). The resist was exposed using standard contact lithography at 365 nm (Karl Suss MA-6). After development, the silicon dioxide was etched in RIE mode using standard recipes [200 W reactive ion etching (RIE) power, 50 SCCM (SCCM denotes cubic centimeters per minute) Ar, 50 sccm CHF_3, and 30 mTorr] in an Oxford Instruments ICP100 system at an etch rate of about 40 nm/min.

III. ETCH CHARACTERISTICS

A. CF_4 and O_2 based etch

Initially we attempted to duplicate the previously reported process for etching of polysiloxanes with CF_4 and Oxygen, but instead used a high density ICP etcher. Etch rates and selectivity were determined from the film thickness measurements before and after 10 min of etching using an SCI Filmtek 4000 which has an accuracy ~10^{-5} for silicalike materials on silicon. Films of 2–5 μm thick were used for this test. Figure 2 shows the etch rate of IPG™ and the selectivity to silicon dioxide as a function of gas mix at 20 W RIE power, 200 W ICP power, 10 mTorr, and 30 SCCM total gas flow. These conditions were previously established to be a reasonable starting point for the etching of a number of different glass systems.

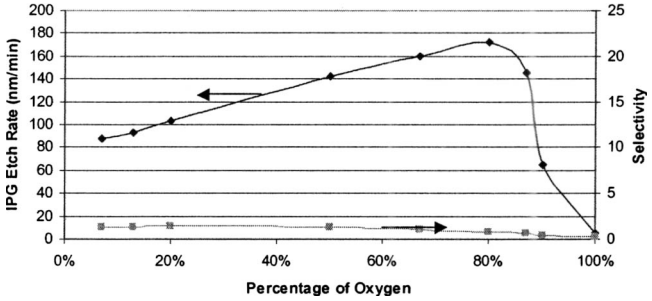

FIG. 2. Etch rate of IPG™ and selectivity against silicon dioxide in CF_4/O_2 gas mixture.

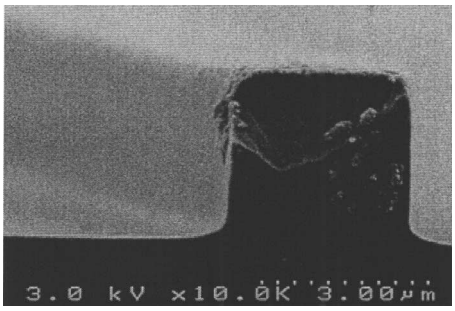

FIG. 4. Electron micrograph of 3 μm wide waveguide etched in 20% CHF_3 in oxygen mix at 10 mTorr, 20 W RIE power, and 200 W ICP power at 30 SCCM total gas flow.

The selectivity was clearly inadequate and, additionally, the etching had a rather less anisotropic character than desired. Also of interest is the very low etch rate of the IPG™ in pure oxygen. This results from the stripping of the organic components, leaving a surface rich in silicon, which is then oxidized to form a protective cap of silicon dioxide thereby vastly reducing the etch rate. Subsequent work, therefore, focused on CHF_3 as the active etch gas. There are two reasons for choosing CHF_3. Firstly, the silica etch rate is strongly influenced by the amount of fluorine in the plasma, and the C–F ratio is lower with CHF_3. Secondly, CHF_3 is known to provide sidewall passivation thereby enhancing etch anisotropy.

B. CHF_3 based etch

The IPG™ etch rate and selectivity to silicon dioxide for a $CHF_3/Ar/O_2$ gas mix were investigated over a wide range of gas compositions and over the available pressure range of the etch system. The RIE power was fixed at 20 W, the ICP power at 200 W. Figure 3 shows the results for the CHF_3/O_2 mix.

Here it is clear that selectivities of up to 25 have been attained at reasonably high etch rates (2.5–3 times that of silica under typical silica etch conditions). It is also interesting to note that only a small amount (13%) of CHF_3 is required for optimum results. Experiments with addition of argon at 20%, 40%, and 60% of the total gas mix all resulted in somewhat poorer selectivities due to the sputtering effect of the argon increasing the silica etch rate significantly. Etched features in the 15%–20% CHF_3 region showed good sidewall verticality and smoothness, as shown in Fig. 4. The roughness of the horizontal etched surfaces was determined using an AFM in tapping mode and was less than 1 nm rms.

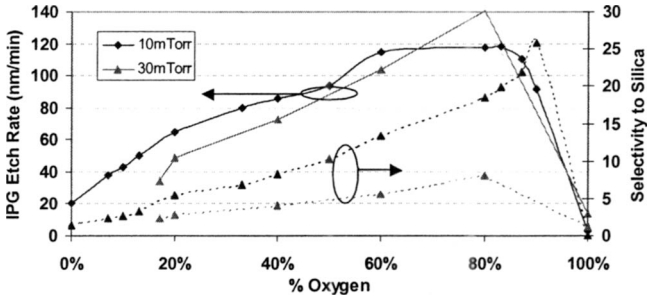

FIG. 3. Etch rate of IPG™ and selectivity to silicon dioxide in CHF_3/O_2 gas mix.

Experimentation with the RIE and ICP powers showed an approximately linear dependence of the etch rate on power with the IPG™ etch rate increasing at ~1.9 nm/min per watt of RIE power, or ~0.35 nm/min per watt of ICP power relative to the baseline 20 W RIE and 200 W ICP powers, respectively. The maximum powers tested were 60 W of RIE and 600 W ICP power, leading to an observed etch rate of 350 nm/min at the maximum powers. However increases in either power from the baseline conditions reported above degraded the selectivity to somewhere in the range of 14–17 dependent on the exact conditions. Additionally we were unable to maintain the vertical profile shown in Fig. 4, and sidewall angles ranged from ~65° to 80° often with recession under the mask edge indicating higher degrees of chemical etching. Therefore the waveguide etching conditions were set as those giving the results in Fig. 4.

IV. WAVEGUIDE FABRICATION

A 13 μm thick underclad of type L3 IPG™ was spin coated and UV cured with a 500 W Hg–Xe lamp filtered to remove any radiation below 300 nm to prevent UV induced damage of the material. This was followed by a 3.7 μm thick core layer of L11 material. The stack was then baked at 180 °C for 3 h. L3 and L11 have refractive indices of 1.502 and 1.531, respectively, at 1550 nm. In this instance, a 250 nm thick layer of PECVD silica was deposited to form the mask using an Oxford Instruments Plasmalab 80 system. The PECVD material was not as high quality as the sputtered material in terms of defects, granularity, and etch resistance. The deposition temperature was 150 °C used with 710 SCCM N_2O, 160 SCCM SiH_4 (5% in N_2), rf power of 20 W, and pressure of 1 Torr. The silica etch mask was then patterned as described above and the waveguides etched 3 μm deep into the core layer thereby creating a deep rib waveguide structure using a 20% CHF_3 gas mix with oxygen. The mask pattern comprised of 9 cm long straight and serpentine structures with three straight sections interconnected by two 180° bends with radii of 2.5–3.2 mm to yield waveguides with a total length of either 17.5 or 24 cm measured to the wafer edge. Line edge roughness on the mask

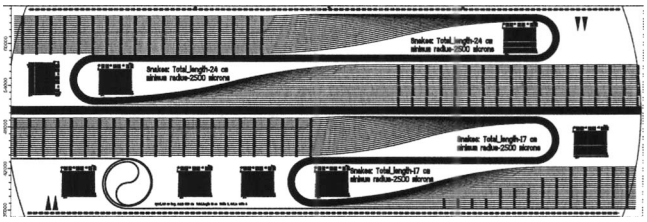

FIG. 5. Snake pattern layout schematic, inner bend radius was 2.5 mm, and outer radius was 3.2 mm.

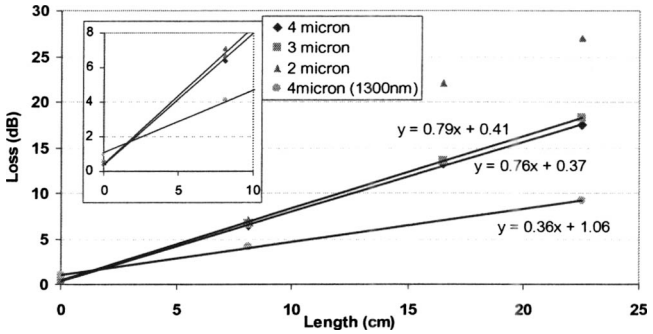

FIG. 6. Waveguide insertion loss data for nominal widths of 2–4 μm. Lines are best linear fit to the raw data. The inset (b) is a magnified view of the 0–8 cm part of the graph showing loss variation as a function of the waveguide width.

(Taiwan Mask Corporation) was measured at 6 nm rms for the straight sections and up to 17 nm rms for curved areas due to discretization of the curves in the deep ultraviolet (DUV) laser writer. Figure 5 shows the mask layout.

Waveguide widths were 4, 3, and 2 μm with five waveguides of each width in the chip. A process bias of −0.2 μm was apparent after etching leaving the waveguides slightly narrower than designed. The etched structures were then overclad with a further 10 μm of IPG™ and hand cleaved with a diamond stylus to leave a chip 8.2 cm long by 3 cm wide containing the straight waveguides and the two different length serpentine patterns.

V. WAVEGUIDE CHARACTERIZATION

Coupling to the waveguides was accomplished using piezocontrolled three axis stages at each end of the waveguide chip and Nufern UHNA-3 fiber to obtain a good mode match. Drops of core IPG™ material without photoinitiator were used on the fiber ends to index match the waveguides, thereby suppressing the effects of reflections and facet imperfections and leaving misalignment and mode overlap as the only sources of coupling loss. Light was injected from either a JDS/FITEL SWS 15101 tunable source at 1550 nm, or a Thorlabs S1-FC-1310 laser for 1310 nm measurements. The source was followed by a scanning polarization controller (Agilent 11896A) to determine polarization dependent loss (PDL), and signal detection was accomplished using a 150 μm diameter SC-receptacled InGaAs detector with low PDL feeding a high accuracy (<0.5% error) six decade logarithmic amplifier (Analog Devices AD757). The output from this was digitized with a 16 bit analog to digital converter card to make measurements.

Figure 6 shows the averaged data collected at 1550 and 1310 nm for waveguides with nominal widths of 2, 3, and 4 μm. The zero length points on the graph represent the calculated mode overlap loss for the actual fabricated waveguide structures to UHNA-3 fiber as calculated using the full vector generic finite difference mode of C2V Olympios and are clearly in excellent agreement with the projected coupling losses. Note that the data for the serpentine waveguides have been corrected for the transition losses associated with the termination of the bends (totaling 0.1 dB), as calculated by BEND2D mode of Olympios.

From the raw data we see that the best fit propagation losses at 1550 nm are 0.76 and 0.79 dB/cm, respectively, for the 4 and 3 μm waveguides, while it is clear that the 2 μm waveguides have suffered significant bending loss as predicted by Bellman *et al.*[7] The 4 μm wide waveguides measured 0.36 dB/cm at 1310 nm.

White light transmission spectra for the 4 μm wide waveguide straights were also recorded, as is shown in Fig. 7(a). Figure 7(b) depicts the excess loss for the waveguides obtained by normalizing out the intrinsic material absorption (from a 1 cm thick block of the cured IPG™ resin as measured on spectrophotometer) and wavelength dependent coupling losses in the 1100–1550 nm range via the known mode field diameter of the UHNA fiber. Outside this range, a parabolic fit was used for extrapolation of the coupling losses. Also shown in Fig. 7(b) is a best fit $1/\lambda^2$ curve which represents the spectral dependence of sidewall scattering.[10]

A clear short wavelength "wall" characteristic of scattering loss is seen, as well as a good fit to the expected spectral

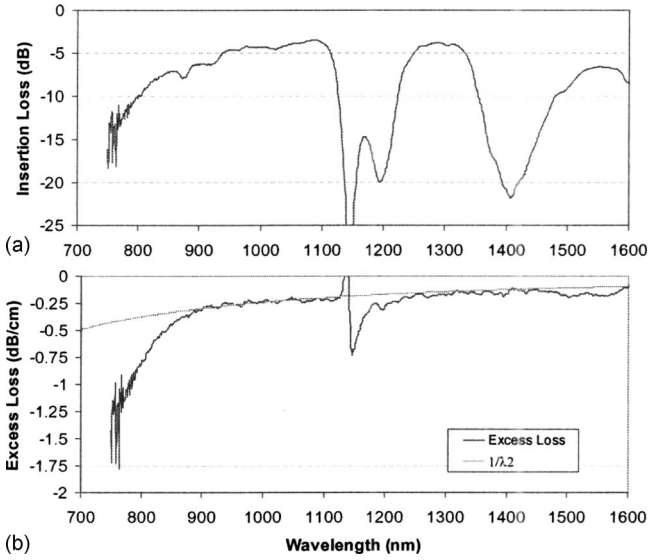

FIG. 7. (a) White light loss spectrum for 8.2 cm long straight waveguide of 4 μm nominal width. (b) Excess loss for the same waveguide where the intrinsic material loss and wavelength dependent coupling loss are normalized out. Also shown is the best fit $1/\lambda^2$ curve representing a fit to sidewall induced scattering losses. Data around 1150 nm are unreliable due to high losses and differences in dynamic range and resolution between instruments used for waveguide and bulk material measurements.

dependence for sidewall scattering losses. The presence of weak scattering losses is also consistent with the trend evident in the inset of Fig. 6 where the losses increase slightly for decreasing waveguide widths. Given the low roughnesses observed during the etch development, the most likely source for this is the use of the PECVD silica mask as this is known to be quite grainy in comparison to the sputtered silica used in the etch development.

Figure 7(b) also clearly identifies a small additional excess loss at 1550 nm of about 0.08 dB/cm. While the exact source of this has proven elusive, one likely source is deep UV induced degradation of the polysiloxane from light generated by the plasma used to etch the waveguide principally from either argon during the mask etch step (though this is very short) or more likely from the fluorocarbon materials or the CO etch products.[15,16] The total excess loss of 0.16–0.19 dB/cm across the telecommunication band is however lower than that reported by Watanabe *et al.*[2] even with the substantially increased index contrast and reduced core size.

Measurements of PDL for the 8.2 cm long straights revealed negligible values for the 4 and 3 μm wide waveguides—indistinguishable from the measurement system background—rising to 0.25 ± 0.015 dB at 2 μm. The PDL rose to values as high as 0.32 dB for the 23 cm long 4 and 3 μm waveguide "snakes." Calculations in the BEND2D mode of Olympios for the actual waveguide structure gave negligible radiation loss and PDL (0.014 and 0.0093 dB/cm for TM/TE in a 2.5 mm radius bend and a 3 μm waveguide). The origin of this additional PDL is unknown but may be associated with tilting of the etched profiles at the bends commonly observed near the wafer periphery.[17] Nevertheless PDL in these structures can be considered to be low.

VI. CONCLUSIONS

We have demonstrated for the first time the production of low loss high index contrast waveguides by reactive ion etching of polysiloxane thin films. The use of a silica mask and CHF_3/O_2 etch gas in optimized conditions led to large etch selectivity between the silica and IPG™ of >20 and etch rates of >100 nm/min. The resulting waveguides showed optical losses in the telecommunication bands dominated by the material loss, although small amounts of excess loss due to scattering and increased material absorption were identifiable. This work indicates that compact optical circuits could be successfully fabricated for telecommunication applications using these polysiloxane materials.

ACKNOWLEDGMENTS

The support of the Australian Research Council through its Linkage grant and Federation Fellow programs is gratefully acknowledged as well as the financial support of RPO Inc.

[1] R. Buestrich, F. Kahlenberg, M. Popall, P. Dannberg, R. Muller-Fiedler, and O. Rosch, J. Sol-Gel Sci. Technol. **20**, 181 (2001).
[2] T. Watanabe, N. Ooba, S. Hayashida, T. Kurihara, and S. Imamura, J. Lightwave Technol. **16**, 1049 (1998).
[3] M. Usui, M. Hikita, T. Watanabe, M. Amano, S. Sugawara, S. Hayashida, and S. Imamura, J. Lightwave Technol. **14**, 2338 (1996).
[4] T. Watanabe, Y. Inoue, A. Kaneko, N. Ooba, and T. Kurihara, Electron. Lett. **33**, 1547 (1997).
[5] T. C. Kowalczyk and R. Blum, Proc. SPIE **5517**, 50 (2004).
[6] W. Norris, J. V. DeGroot, T. Ogawa, T. Watanabe, T. C. Kowalczyk, A. Baugher, and R. Blum, Proc. SPIE **5212**, 76 (2003).
[7] R. A. Bellman, G. Bourdon, G. Alibert, A. Beguin, E. Guiot, L. B. Simpson, P. Lehuede, L. Guiziou, and E. LeGuen, J. Electrochem. Soc. **151**, G541 (2004).
[8] K. K. Lee, D. R. Lim, H. C. Luan, A. Agarwal, J. Foresi, and L. C. Kimerling, Appl. Phys. Lett. **77**, 1617 (2000).
[9] R. Charters, personal communication (April, 1 2004).
[10] P. K. Tien, Appl. Opt. **10**, 2395 (1971).
[11] D. Szmigiel, K. Domański, P. Prokaryn, P. Grabiec, and J. Sobczak, Appl. Surf. Sci. **253**, 1506 (2006).
[12] D. Szmigiel, K. Domański, P. Prokaryn, and P. Grabiec, Microelectron. Eng. **83**, 1178 (2006).
[13] T. Ohzono and M. Shimomura, Phys. Rev. E **72**, 025203 (2005).
[14] See http://web.mit.edu/6.777/www/matprops/pecvd_sio2.htm
[15] H. J. Tao, C. S. Tsai, B. L. Lin, C. W. Su, S. P. Lin, Y. C. Huang, and S. C. Sun, Proceedings of the Third Internation Symposium Plasma Process-Induced Damage, Honolulu, HI, 4–5 June 1998 (unpublished), pp. 60–63.
[16] S. Lee, Y.-C. Tien, and C.-F. Hsu, J. Vac. Sci. Technol. B **18**, 805 (2000).
[17] M. Jansen, M. de Boer, and M. Elwenspoek, Proceedings of the Micro Electro Mechanical Systems (MEMS '96), San Diego, CA, 11–15 February 1996 (unpublished), pp. 250–257.